

Reduction of Neoclassical Transport and Observation of a Fast Electron Driven Instability with Quasisymmetry in HSX

J.M. Canik 1), D.L. Brower 2), C. Deng 2), D.T. Anderson 1), F.S.B. Anderson 1), A.F. Almagri 1), W. Guttenfelder 1), K.M. Likin 1), H.J. Lu 1), S. Oh 1), D.A. Spong 3), J.N. Talmadge 1)

1) University of Wisconsin at Madison, Madison, Wisconsin, USA

2) University of California at Los Angeles, Los Angeles, California, USA

3) Oak Ridge National Laboratory, Oak Ridge, Tennessee, USA

email contact of main author: canik@cae.wisc.edu

Abstract. The Helically Symmetric Experiment (HSX) is the first operational quasisymmetric stellarator, with neoclassical transport at low collisionality greatly reduced compared to a conventional stellarator. Experimental differences in the density and temperature profiles are observed between the quasihelically symmetric (QHS) configuration and a configuration with the symmetry intentionally broken. The central electron temperature in the QHS configuration is significantly higher than in the non-symmetric configuration with the same launched power. The density profile in the QHS configuration is always centrally peaked, regardless of heating location, whereas in the non-symmetric configuration the core density profile is flattened with central heating. Transport analysis shows that this flattening is due to neoclassical thermodiffusion, which is reduced in the QHS configuration. Measurements show that the thermal conductivity is reduced in the QHS configuration by an amount comparable to the neoclassical reduction. An unexpected consequence of the improved confinement in the QHS configuration is that a fast particle population drives an Alfvénic instability. We report on experimental observations of a fast electron driven Alfvénic mode in QHS plasmas. These modes are coherent and global, peaking in the plasma core. The measured frequency range, propagation direction, and scaling with ion mass density are consistent with theoretical predictions for the Global Alfvén Eigenmode. When symmetry is broken, the mode is no longer observed.

1. Introduction

The Helically Symmetric Experiment [1] (HSX) is the first operational quasisymmetric stellarator, with a helical direction of symmetry in the magnetic field strength. As a result of this symmetry, the neoclassical transport is reduced to the level of an axisymmetric device. HSX is a medium sized device, with a major radius of 1.2 m and a minor radius of 12 cm. The quasihelically symmetric (QHS) magnetic field, with a toroidal mode number of $n=4$ and poloidal mode number of $m=1$, is produced with 48 non-planar modular coils. The symmetry can be intentionally broken using a set of auxiliary coils, which add toroidal mirror terms with mode numbers $(n=4, m=0)$ and $(n=8, m=0)$ to the magnetic spectrum. In this configuration, called Mirror, the level of neoclassical transport is raised back towards the level of a conventional stellarator. Plasmas in HSX are produced and heated with up to 100 kW of 2nd harmonic electron cyclotron resonance heating (ECRH) at 28 GHz, at a magnetic field strength of 0.5 T. This produces plasmas with low density and high electron temperatures, allowing low-collisionality transport to be studied as a function of the magnetic spectrum. This paper presents the first experimental demonstration of reduced particle and heat transport due to quasisymmetry. Also reported are measurements of Alfvénic activity driven by energetic electrons, which are well confined in the symmetric field.

2. Particle Transport

In order to study particle transport in HSX plasmas, Thomson Scattering is used to measure the electron temperature and density profiles [2]. This system has 10 spatial channels with 2

cm resolution along a 20 cm laser beam path. The density is also measured with a 9-chord microwave interferometer [3]. The particle source is measured using a suite of absolutely calibrated H_α detectors [4], with an array covering the plasma cross-section and several detectors distributed toroidally around the machine. The data from the H_α suite is interpreted using neutral gas modeling with the DEGAS code [5]. DEGAS is a three-dimensional Monte Carlo neutral gas code, which takes as its input the 3D plasma geometry and profiles, and for a given gas puff yields the line-integrated H_α signal for each of the detectors. The input gas rate is then adjusted so that the calculated H_α level agrees with one of the detectors. This results in good agreement between the profiles of the H_α brightness calculated from DEGAS and that from the rest of the detectors [6]. From the DEGAS code, the particle source rate density is calculated, and then integrated to give the total radial particle flux.

The temperature and density profiles for both QHS and Mirror plasmas are shown in Fig. 1. The measurements shown are from the Thomson scattering system. These plasmas are heated with 80 kW of ECRH. It can be seen that the electron temperature is substantially higher in the QHS case; this will be the topic of the next section. The density profiles in the two configurations are also quite different: the profile in the QHS plasma is centrally peaked, whereas that in the Mirror configuration is hollow in the core. The measurement of a hollow density profile has been independently corroborated by interferometry. To support a hollow density profile in steady state requires an outward convective flux in addition to the particle flux driven by the density gradient.

The neoclassical particle flux has been calculated for the Mirror case and compared to the experimental flux inferred from the H_α measurements. The neoclassical transport coefficients have been calculated for the Mirror configuration using the DKES code [7,8]. The electric field has been solved for self-consistently using the ambipolarity constraint on the neoclassical particle fluxes. The resulting neoclassical flux is shown in Fig. 2, along with the experimental value. It can be seen that in the region of hollow density profile ($r/a < 0.4$), the experimental and neoclassical particle fluxes are comparable. Flux driven by the temperature gradient is the dominant component of the total

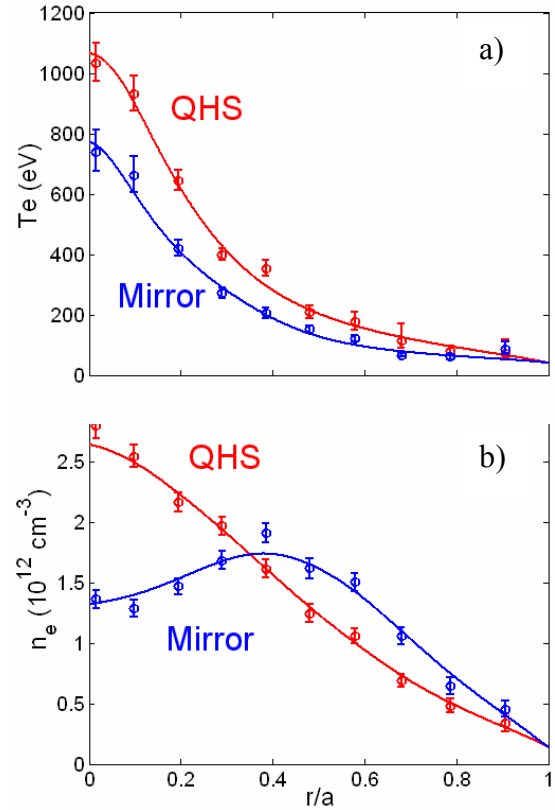


Figure 1: Profiles of a) electron temperature and b) density in QHS and Mirror plasmas

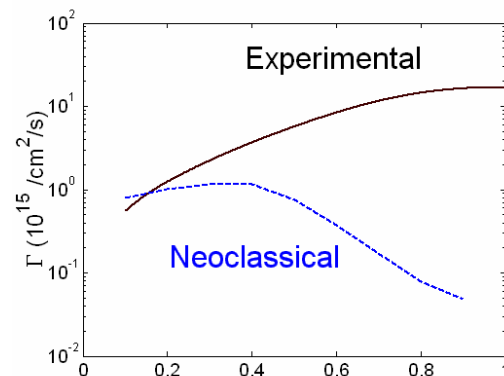


Figure 2: Experimental and neoclassical particle fluxes for the Mirror discharge shown in Fig. 1.

neoclassical particle flux; in fact it accounts for all of the outward directed flux in the core, as the density gradient drives an inward flux in this region. This shows that neoclassical thermodiffusion causes the hollow density profiles observed in the Mirror configuration. This is very similar to results from other stellarators, in which hollow density profiles were attributed to neoclassical thermodiffusion [9]. That thermodiffusion causes the hollow profiles is also supported by off-axis heating experiments, in which the core temperature profile is flattened: when the temperature gradient is reduced the density profile in the Mirror configuration becomes centrally peaked. In QHS plasmas, the neoclassical particle flux is greatly reduced compared to the Mirror case, due to quasisymmetry. This reduction includes the thermodiffusive component. As can be seen in Fig. 1, a consequence of the reduction in neoclassical thermodiffusion is that the density profile is centrally peaked.

3. Electron Heat Transport

The higher electron temperature in QHS plasmas as shown in Fig. 1 indicates an improvement in heat transport. However, these plasmas are not ideal for comparing differences in thermal transport to neoclassical predictions, as these differences could be masked by a temperature dependence in the anomalous transport. To overcome this, discharges have been studied in which the temperature profiles in the two configurations are similar. This is accomplished by heating the Mirror plasma with 70 kW of ECRH power, and lowering the power in the QHS case to 25 kW. The temperature and density profiles of these plasmas are shown in Fig. 3. Note that although the temperatures in the two configurations are very similar, the large thermodiffusive flux in Mirror makes it impossible to match the density in the same way.

In order to perform a transport analysis on these discharges, the total power absorbed by the plasma has been measured using the Thomson scattering system. This was done by taking many similar discharges, and varying the time at which the Thomson measurement is made from just before to just after the turn-off of the ECRH power. At each time point, the kinetic stored energy is calculated from the density and temperature profiles. The absorbed power is then obtained from the rate at which the energy decays just after turn-off, similar to the way in which absorbed power measurements are made using a diamagnetic loop to measure the stored energy. The reason for using this method rather than the diamagnetic measurements routinely made on HSX is that the diamagnetic stored energy is often contaminated by the

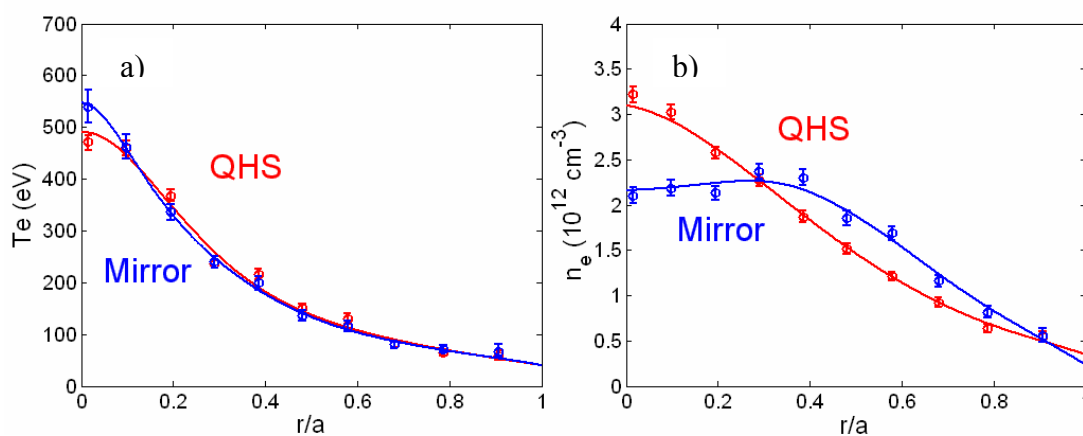


Figure 3: Profiles of a) electron temperature and b) density for QHS discharges with 25 kW of injected power and Mirror discharges with 70 kW of power.

presence of a high-energy electron tail [10]. This population can dominate the total stored energy and absorbed power, especially at higher launched power. Since the Thomson scattering measurements are less sensitive to the high-energy tail, they are a better measurement of the bulk energy and absorbed power.

In the low power QHS discharges, the tail population is low; the absorbed power thus measured is 10 kW, which is in fair agreement with the diamagnetic value of 15 kW. In the high power Mirror discharge, however, the absorbed power from the Thomson scattering method is 15 kW, compared to 38 kW from the diamagnetic loop. The kinetic stored energy in both configurations is 17 J, giving bulk confinement times of 1.7 ms for the QHS plasma and 1.1 ms for Mirror. It should be noted that the absorbed power has been obtained by measuring the drop in kinetic stored energy over 400 μ s after the ECRH turn-off. This time increment is too large compared to the energy confinement times to accurately measure the absorbed power, and so the power will tend to be underestimated by this method. This effect is larger in the Mirror configuration however, as the confinement time is smaller, and the difference between transport in QHS and Mirror plasmas is likely somewhat larger than that reported here.

An analysis of electron heat transport has been performed for the QHS and Mirror plasmas shown in Fig. 3. In this analysis, a model profile shape for the power absorption has been used, and the total power is taken from the measurements made with the Thomson scattering system. The shape of the absorbed power profile is based on ray tracing calculations, which show very centrally peaked power deposition, with negligible difference in shape between the QHS and Mirror cases. A purely conductive ansatz is used for the electron heat transport, with $q_e = -n_e \chi_e \nabla T_e$. This is not valid outside a minor radius of $r/a \sim 0.7$, where convection and radiation make up a significant part of the electron power balance. These are negligible in the core, however, as is power transfer from electrons to the ions.

The results of this analysis are shown in Fig. 4, where the experimental electron thermal diffusivity χ_e is shown in the plasma core. The error bars shown in the graph are taken from both the error in the measurement of the temperature profiles, and from the error in the kinetic measurement of the absorbed power. It can be seen from this figure that the transport in the two plasmas is similar towards the edge, and the QHS transport is reduced in the core compared to the Mirror case. At a radius of $r/a \sim 0.2-0.3$, where the temperature gradient is well determined, the value of χ_e is just above 2 m^2/s in QHS, and $\sim 4 \text{ m}^2/\text{s}$ in Mirror. Also shown are the neoclassical values of the thermal diffusivity. The neoclassical thermal diffusivity is calculated assuming a Maxwellian plasma, which may not be appropriate. The magnitude of the reduction in the experimental χ_e in QHS compared to Mirror is comparable to the reduction in the neoclassical value. Towards the edge of the plasma, where the neoclassical transport is small compared to experiment, the two configurations have

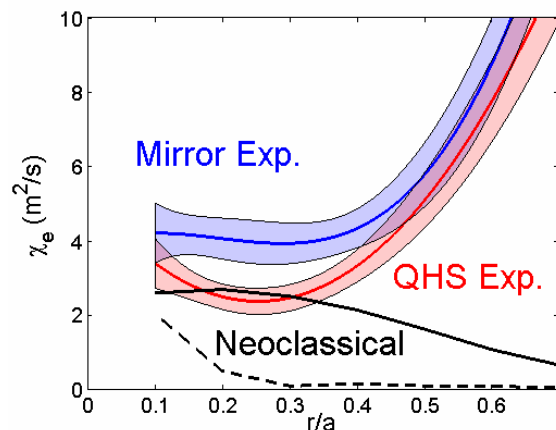


Figure 4: Thermal diffusivities for the discharges shown in Fig. 3. Solid black line is the Mirror neoclassical value, dashed black is QHS neoclassical.

similar values of χ_e . These results demonstrate reduced electron heat transport due to the low neoclassical transport with quasisymmetry.

4. Alfvénic Mode Activity

Alfvén instabilities driven by energetic ions have been observed in several experiments on tokamaks [11-15] as well as stellarators [16-18]. These energetic ions are produced by neutral-beam injection (NBI) or ion cyclotron resonance heating. The effect of Alfvén eigenmodes (AE) on plasma confinement and machine operation is of great interest to the fusion community as they may impact the performance of future reactor relevant devices. The resonance condition for passing particles requires velocity of order or greater than the Alfvén velocity [$v_A = B/(4\pi n_i m_i)^{1/2}$, where $n_i m_i$ is the ion mass density] and the mode is driven unstable through the inverse Landau damping process when $\omega_p^* > \omega$, where ω is the Alfvénic mode frequency and ω_p^* is the diamagnetic drift frequency of the energetic particle species. In addition, trapped energetic particles with a precessional drift frequency matching the mode frequency can also excite an instability. In both cases, a basic feature of the resonance is that it requires the particles have a specific energy, not mass. Thus, in theory, energetic electrons are able to drive fast particle instabilities just as effectively as energetic ions. As mentioned in the previous section, the ECRH used to heat HSX plasmas produces a population of highly energetic electrons. Here we report on the first experimental evidence for fast-electron-driven Alfvénic modes in quasi-helically symmetric HSX plasmas. Such modes have previously been observed in both tokamaks and stellarators but have always been driven by energetic ions, not electrons. In HSX, instability is only observed for QHS plasmas and has been identified as a Global Alfvén Eigenmode (GAE). When a toroidal mirror term is introduced into the magnetic field spectrum, the Alfvénic fluctuation is no longer observed. Measurements presented in this paper provide two new results; (1) fast electrons can drive Alfvénic instabilities, and (2) quasi-symmetry makes a difference, perhaps by better confining the particles that drive the instability as compared to the conventional stellarator configuration. These results contribute to a broader understanding of Alfvénic instabilities in toroidal devices.

Temporal evolution of a typical QHS discharge ($\bar{n}_e \approx 1.5 \times 10^{12} \text{ cm}^{-3}$) is shown in Fig. 5, where 100 kW of ECRH power terminates at ~ 30 ms. During the ECRH pulse, a single coherent mode is observed at frequency ~ 50 kHz on the electron density time series trace as measured by interferometry. This mode is also observed on a set of magnetic pickup coils. After ECRH turn-off, the mode decays on a timescale (~ 0.2 ms) much faster than the energy confinement time (~ 1 ms) as estimated from the stored energy. A characteristic feature of 2nd harmonic X-mode ECRH is the generation of fast electrons with high perpendicular velocities ($T_{e\perp} \gg T_{e\parallel}$) as evidenced by electron

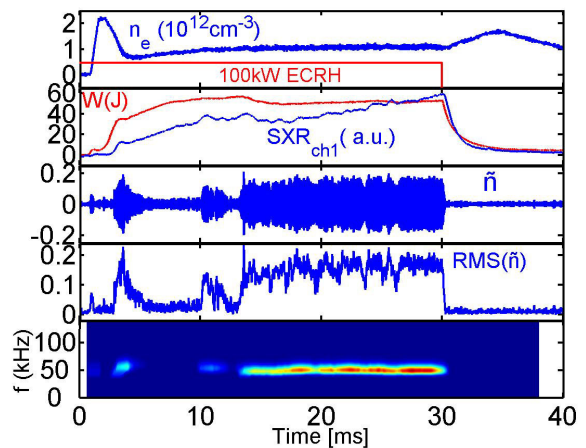


Figure 5: Time series traces showing electron density, stored energy W_{dia} , soft x-ray emission, and electron density fluctuations for a QHS HSX plasma. $P_{ECRH} = 100 \text{ kW}$.

cyclotron emission (ECE), x-ray, and stored energy measurements [10,19]. For example, ECE measurements of electron temperature are significantly larger than Thomson scattering results, especially at lower densities $\bar{n}_e \leq 1.5 \times 10^{12} \text{ cm}^{-3}$ [20]. In addition, stored energy from diamagnetic loops is larger than that determined using Thomson scattering measurements, as mentioned previously. Both these results support the notion that energetic electrons are available to drive instability. There is no source for fast ions.

Spatial information from the 9-channel interferometer shows the mode has an $m=1$ nature as a π -phase change is clearly seen across the magnetic axis (see Fig. 6(a)). Toroidally displaced Langmuir probe measurements indicate the mode has toroidal mode number $n=1$. The density fluctuation spatial distribution is determined by inverting the interferometer data using the known helicity. As shown in Fig. 6(b), the mode is global, peaking in the plasma core near $r/a=0.4$ where the density gradient is steepest. The mode amplitude is $\tilde{n}/n_e \approx 4 \times 10^{-3}$ ($r/a=0.4$) and the magnetic perturbation is $\tilde{B}_\theta/B \approx 4 \times 10^{-5}$ at the wall. The mode propagates in the electron diamagnetic drift direction. When the ECRH heating power is at or above 100 kW, the stored energy is degraded up to 15% with appearance of the mode as shown in Fig. 5 beginning at ~ 14 msec.

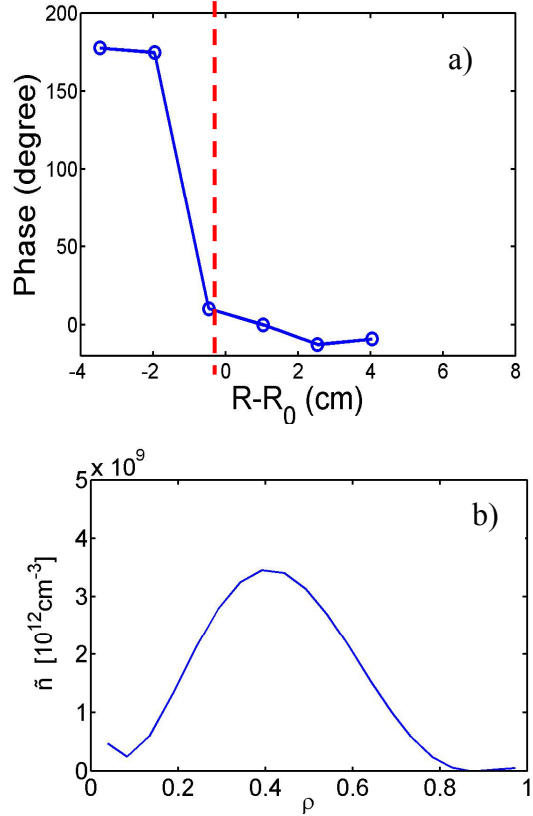


Figure 6: Density perturbation (a) phase, and (b) spatial distribution profiles.

Theoretical calculations obtained from the STELLGAP code [21] using the HSX QHS equilibrium show a gap exists beneath the Alfvén continuum for an $m=1$, $n=1$ Global Alfvén Eigenmode (GAE) in the spectral region where the fluctuations are experimentally observed. GAE modes with discrete frequencies $\omega_{GAE} \leq k_{\parallel} v_A \equiv \omega_A$ [parallel wave number $k_{\parallel} = (m\ell - n)/R$] are predicted and found consistent with the measured fluctuations. Fluctuations with frequency 20-120 kHz in the laboratory frame are observed and scaling with ion mass density matches the expected $(m_i n_i)^{-1/2}$ dependence for Alfvénic modes. This is evident in Fig. 7, where the measured mode frequency density scaling is shown for a variety of working gases. Note that at lower densities, a satellite mode is observed with an upshifted frequency of ~ 20 kHz.

A distinguishing feature of these fluctuations is that they are only observed for quasi-helically symmetric HSX plasmas. Introduction of a toroidal mirror term in the magnetic field spectrum acts to degrade the helical symmetry. The measured Alfvénic mode amplitude is found to be sensitive to the mirror perturbation and rapidly decreases with its introduction. Only a 2% perturbation of the main coil ampere-turns in the auxiliary coils is required to

eliminate the Alfvénic mode. The STELLGAP code predicts a gap for the Mirror configuration in HSX that is similar to that for QHS operation.

The observed difference between QHS and non-symmetric HSX plasmas can potentially be explained by enhanced particle losses. In addition to improved confinement for thermal particles in the QHS configuration, evidence also exists for improved energetic particle confinement. This is supported by significantly higher x-ray fluxes for QHS as compared to Mirror plasmas [22]. A direct connection between the energetic particles resonant with the mode and improved confinement remains to be established although it is predicted that direct orbit losses of energetic trapped particles, likely generated by ECRH in HSX, should be greatly reduced for the quasi-helically symmetric configuration.

5. Conclusions

The effects of the quasisymmetry in HSX have been observed to affect both particle and electron heat transport. Due to the reduced neoclassical thermodiffusion, QHS plasmas have centrally peaked density profiles, in contrast to the hollow profiles observed when the symmetry is broken. Additionally, higher electron temperatures are achieved in QHS plasmas for a fixed input power. Experiments with matched temperature profiles indicate that the heat transport in QHS plasmas is lower than in Mirror by an amount consistent with the neoclassical predictions. These results demonstrate that reducing neoclassical transport through quasisymmetry leads to reduced experimental transport. An unexpected consequence of the improved confinement in the QHS configuration is that an Alfvénic instability driven by fast electrons is experimentally observed for the first time. The mode is coherent and global, peaking in the plasma core, and has characteristics consistent with Global Alfvén Eigenmodes. When symmetry is broken, the mode is no longer observed.

References

- [1] F.S.B. Anderson et al., *Fusion Technol.* **27**, 273 (1995).
- [2] K. Zhai et al., *Rev. Sci. Instrum.* **75**, 3900 (2004).
- [3] C. Deng et al., *Rev. Sci. Instrum.* **74**, 1625 (2003).
- [4] S.P. Gerhardt et al., *Rev. Sci. Instrum.* **75**, 2981 (2004).
- [5] D. Heifetz et al., *J. Comp. Phys.* **46**, 309 (1982).
- [6] J. Canik et al., 14th International Stellarator Workshop, Greifswald 2003.
- [7] S.P. Hirshman et al., *Phys. Fluids* **29**, 2951 (1986).
- [8] W.I. van Rij and S.P. Hirshman, *Phys. FluidsB* **1**, 563 (1989).
- [9] H. Maassberg et al., *Plasma Phys. Control. Fusion* **35**, B319 (1993).

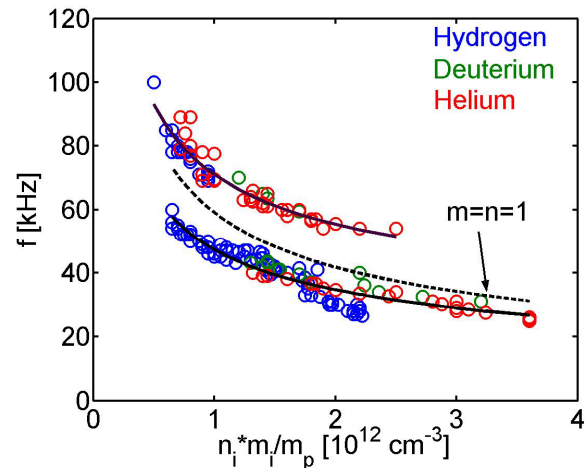


Figure 7: Scaling of mode frequency with ion mass density. Measured mode frequency, in the laboratory frame, is denoted by open circles. Solid lines denote $(m_i n_i)^{-1/2}$ scaling and dashed line represents calculated Alfvén continuum for $n=1, m=1$.

- [10] K.M. Likin et al., Plasma Phys. Control. Fusion **45**, A133 (2003).
- [11] E.D. Fredrickson, et al., Phys. Rev. Lett. **87**,145001 (2001).
- [12] S.E. Sharapov, et al., Phys. Rev. Lett. **93**,125003 (2004).
- [13] R. Nazikian, et al., Phys. Rev. Lett. **91**,165001 (2003).
- [14] M.A. Van Zeeland, et al., Plasma Phys. Contr. Fusion **47**,L31-L40(2005).
- [15] K.L. Wong, et al., Phys. Rev. Lett. **66**,1874 (1992). K.L. Wong et al., Plasma Phys. Control. Fusion **41**, R1(1999).
- [16] A. Weller et al., Phys. Rev. Lett. **72**,1220 (1994).
- [17] M. Takechi, et al., Phys. Rev. Lett. **83**,312 (1999).
- [18] S. Yamamoto, et al., Phys. Rev. Lett. **91**,245001 (2003).
- [19] S. Morimoto et al., Nucl. Fusion **29**,1697 (1989).
- [20] K.M. Likin, et al., Bull. APS 46th Annual Meeting of DPP, **49**,PP1.041 (2004).
- [21] D. Spong, R. Sanchez, A. Weller, Phys. Plasmas **10**,3217 (2003).
- [22] S.P. Gerhardt et al., Proc. 19th IAEA Fusion Energy Conference (Lyon, 2002) IAEA-CN-94/EX/P3-22.